Mechanisms of K^+ coupling in the glutamate transporter family

Daniel Kortzak[1], Claudia Alleva[1], David Ewers[2], Ingo Weyand[1], Jan-Philipp Machtens[1], Christoph Fahlke[1]

[1]ICS-4, Forschungszentrum Jülich, Germany, [2]Abteilung für Neurogenetik, Max-Planck-Institut für experimentelle Medizin, Göttingen, Germany.

JÜLICH Forschungszentrum

Introduction

Glutamate uptake by mammalian excitatory amino acid transporters (EAATs) is driven by the stoichiometrically coupled co-transport of three Na^+ and one H^+ with the antiport of one K^+ [1]. Related bacterial and prokaryotic transporters use Na^+ cotransport only [2]. X-ray crystal structures of the prokaryotic homolog Glt_{Ph} [3] and of human EAAT1 [4] have illuminated mechanisms of Na^+ and glutamate/aspartate binding and revealed a elevator transport mechanism. Glutamate is transported via alternating inward- and outward-directed rigid-body motions of the mobile transport domain, either bound to (i) glutamate, and three Na^+, and one H^+ or to (ii) one K^+. The recently resolved structure of EAAT1 bound to Na^+ and aspartate did not uncover the molecular basis of K^+-coupled glutamate transport. We combined molecular dynamics (MD) simulations of Glt_{Ph} and human EAAT1 with experiments on Glt_{Ph}, EAAT1 and EAAT2 to identify the K^+-coupling mechanism of EAATs.

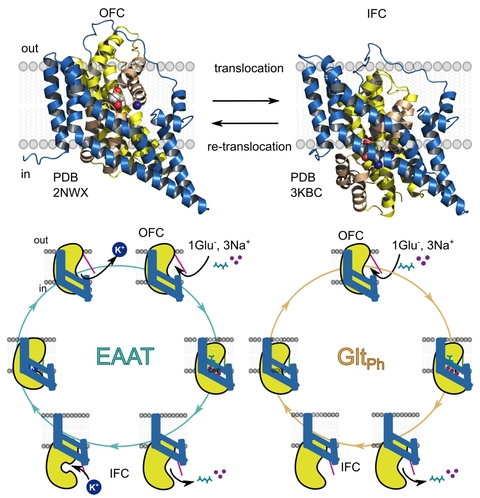

1. Unguided MD simulations identify conserved K^+-binding sites in EAAT1 and Glt_{Ph}

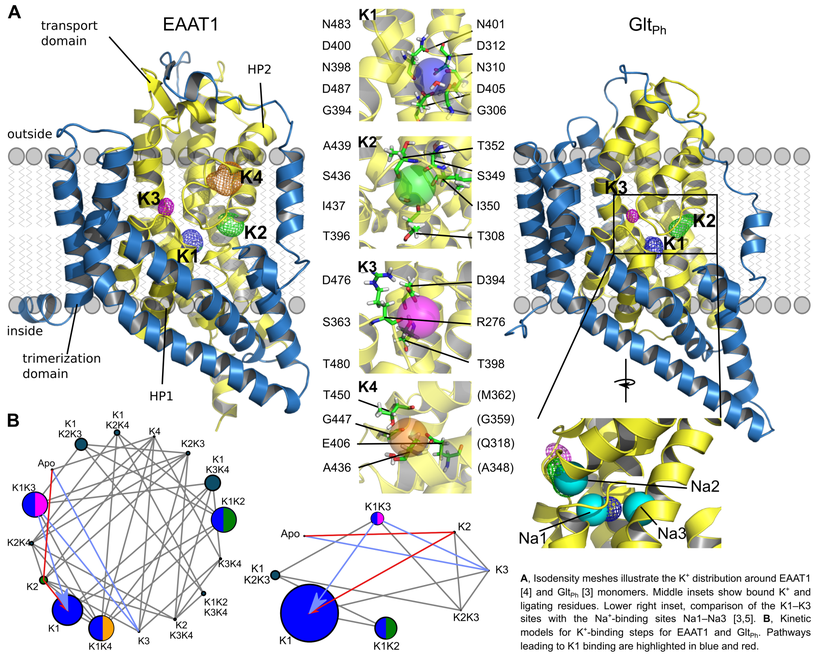

A, Isodensity meshes illustrate the K^+ distribution around EAAT1 [4] and Glt_{Ph} [3] monomers. Middle insets show bound K^+ and ligating residues. Lower right inset, comparison of the K1–K3 sites with the Na^+-binding sites Na1–Na3 [3,5]. **B**, Kinetic models for K^+-binding steps for EAAT1 and Glt_{Ph}. Pathways leading to K1 binding are highlighted in blue and red.

2. The K1 site is conserved between EAATs/Glt_{Ph} and responsible for K^+-bound re-translocation

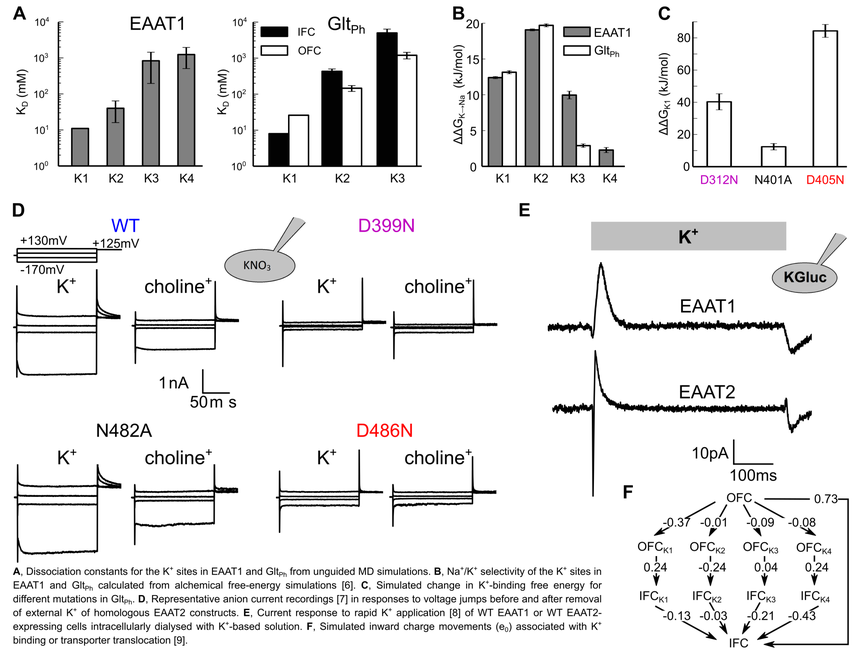

A, Dissociation constants for the K^+ sites in EAAT1 and Glt_{Ph} from unguided MD simulations. **B**, Na^+/K^+ selectivity of the K^+ sites in EAAT1 and Glt_{Ph} calculated from alchemical free-energy simulations [6]. **C**, Simulated change in K^+-binding free energy for different mutations in Glt_{Ph}. **D**, Representative anion current recordings [7] in responses to voltage jumps before and after removal of external K^+ of homologous EAAT2 constructs. **E**, Current response to rapid K^+ application [8] of WT EAAT1 or WT EAAT2-expressing cells intracellularly dialysed with K^+-based solution. **F**, Simulated inward charge movements (e_0) associated with K^+ binding or transporter translocation [9].

3. K1 binding closes the extracellular gate and facilitates re-translocation

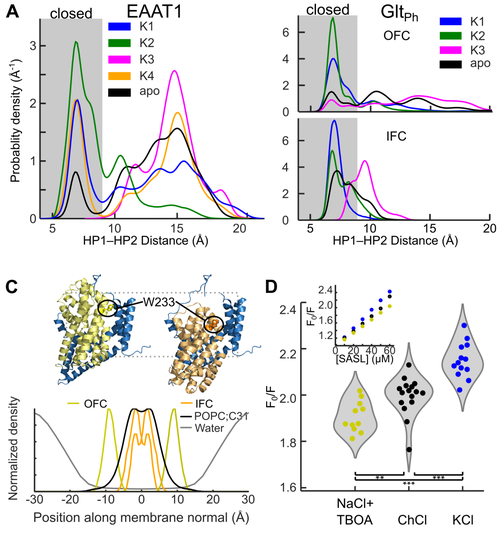

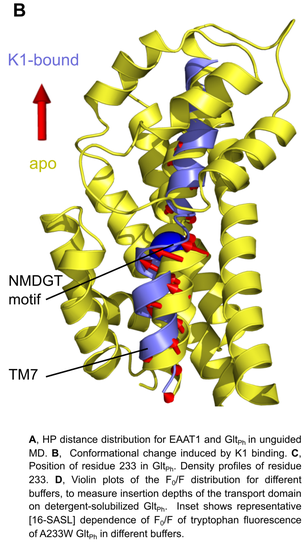

A, HP distance distribution for EAAT1 and Glt_{Ph} in unguided MD. **B**, Conformational change induced by K1 binding. **C**, Position of residue 233 in Glt_{Ph}. Density profiles of residue 233. **D**, Violin plots of the F_0/F distribution for different buffers, to measure insertion depths of the transport domain on detergent-solubilized Glt_{Ph}. Inset shows representative [16-SASL] dependence of F_0/F of tryptophan fluorescence of A233W Glt_{Ph} in different buffers.

4. Stabilizing the closed gate renders EAATs K^+ independent

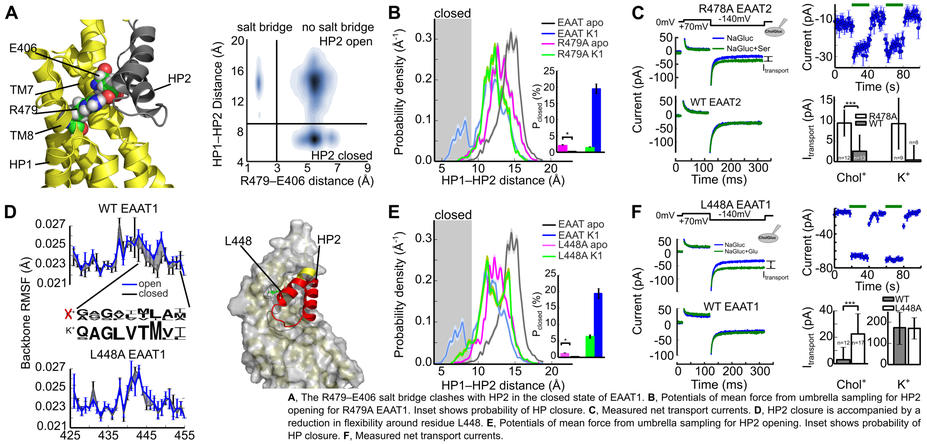

A, The R479–E406 salt bridge clashes with HP2 in the closed state of EAAT1. **B**, Potentials of mean force from umbrella sampling for HP2 opening for R479A EAAT1. Inset shows probability of HP closure. **C**, Measured net transport currents. **D**, HP2 closure is accompanied by a reduction in flexibility around residue L448. **E**, Potentials of mean force from umbrella sampling for HP2 opening. Inset shows probability of HP closure. **F**, Measured net transport currents.

Conclusions

- K^+ binding to the conserved K1 site closes the extracellular gate HP2
- Gate closure is required for transmembrane translocation
- Differences in gate free-energy landscapes result in distinct K^+:gate coupling efficacies [10] $\alpha = \frac{K^+_{half,close}}{K^+_{half,open}}$
  - $\alpha_{Glt_{Ph}}$=20 → K^+-independent transport
  - α_{EAATs}=114 → obligate K^+ coupling
- Allosteric K^+ coupling permits adaptation of the transport stoichiometry without interfering with substrate binding.

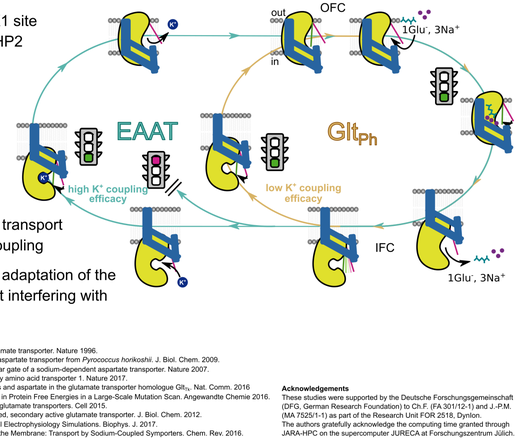

References

[1] Zerangue, N. & Kavanaugh, M. P. Flux coupling in a neuronal glutamate transporter. Nature 1996.
[2] Ryan, R. M. et al. Functional characterization of a Na^+-dependent aspartate transporter from *Pyrococcus horikoshii*. J. Biol. Chem. 2009.
[3] Boudker, O. et al. Coupling substrate and ion binding to extracellular gate of a sodium-dependent aspartate transporter. Nature 2007.
[4] Canul-Tec, J. C. et al. Structure and allosteric inhibition of excitatory amino acid transporter 1. Nature 2017.
[5] Guskov, A. et al. Coupled binding mechanism of three sodium ions and aspartate in the glutamate transporter homologue Glt_{Ph}. Nat. Comm. 2016
[6] Gapsys, V. et al. Accurate and Rigorous Prediction of the Changes in Protein Free Energies in a Large-Scale Mutation Scan. Angewandte Chemie 2016.
[7] Machtens, J. P. et al. Mechanisms of anion conduction by coupled glutamate transporters. Cell 2015.
[8] Grewer, C. et al. Charge compensation mechanism of a Na^+-coupled, secondary active glutamate transporter. J. Biol. Chem. 2012.
[9] Machtens, J. P. et al. Gating Charge Calculations by Computational Electrophysiology Simulations. Biophys. J. 2017.
[10] LeVine M. et al. Allosteric Mechanisms of Molecular Machines at the Membrane: Transport by Sodium-Coupled Symporters. Chem. Rev. 2016.

Acknowledgements

These studies were supported by the Deutsche Forschungsgemeinschaft (DFG, German Research Foundation) to Ch.F. (FA 307/12-1) and J.-P.M. (MA 7525/1-1) as part of the Research Unit FOR 2518, DynIon.
The authors gratefully acknowledge the computing time granted through JARA-HPC on the supercomputer JURECA at Forschungszentrum Jülich.